



Hydrogeochemistry of prairie pothole region wetlands: Role of long-term critical zone processes[☆]

Martin B. Goldhaber^{a,*}, Christopher T. Mills^b, Jean M. Morrison^b, Craig A. Stricker^c, David M. Mushet^d, James W. LaBaugh^e

^a U.S. Geological Survey, Crustal Science Center, MS 964, Denver Federal Center, Denver, CO 80224, United States

^b U.S. Geological Survey, MS 964, Denver Federal Center, Denver, CO 80224, United States

^c U.S. Geological Survey, MS 963, Denver Federal Center, Denver, CO 80224, United States

^d U.S. Geological Survey, 8711 37th Street SE, Jamestown, ND 58401, United States

^e U.S. Geological Survey, MS 411, Reston, VA, United States

ARTICLE INFO

Article history:

Received 15 April 2014

Received in revised form 19 August 2014

Accepted 20 August 2014

Available online 28 August 2014

Editor: Carla M. Koretsky

Keywords:

Prairie pothole region
Wetland sulfur geochemistry
Wetland geochemistry
Cottonwood Lake
Stutsman County, ND
Kidder County, ND

ABSTRACT

This study addresses the geologic and hydrogeochemical processes operating at a range of scales within the prairie pothole region (PPR). The PPR is a 750,000 km² portion of north central North America that hosts millions of small wetlands known to be critical habitat for waterfowl and other wildlife. At a local scale, we characterized the geochemical evolution of the 92-ha Cottonwood Lake study area (CWLSA), located in North Dakota, USA. Critical zone processes are the long-term determinant of wetland water and groundwater geochemistry via the interaction of oxygenated groundwater with pyrite in the underlying glacial till. Pyrite oxidation produced a brown, iron oxide-bearing surface layer locally over 13 m thick and an estimated minimum of 1.3×10^{10} g sulfate (SO_4^{2-}) at CWLSA. We show that the majority of this SO_4^{2-} now resides in solid-phase gypsum ($\text{CaSO}_4 \cdot 2\text{H}_2\text{O}$) and gypsum-saturated groundwater.

Results from the CWLSA were scaled up to a 9700 km² area surrounding CWLSA using ~1800 drill logs and literature data on wetland water chemistry for 178 wetlands within this larger area. The oxidized brown zone depth and wetland water compositional trends are very similar to the CWLSA. Additionally, surface water data from 176 southern Canadian pothole wetlands that conform to the same wetland water geochemical trends as those recorded in the CWLSA further corroborate that SO_4^{2-} accumulation driven by pyrite oxidation is a nearly ubiquitous process in the prairie pothole region and distinguishes PPR wetlands from other wetlands worldwide that have a similar overall hydrology.

Published by Elsevier B.V.

1. Introduction

The National Research Council's (NRC) Committee on Basic Research Opportunities in the Earth Sciences (2001) defines the critical zone as the external surface of the Earth extending from the outer limits of vegetation down to, and including, the zone of groundwater. More recently, the critical zone concept has been amended to increase emphasis on the role of geologic history in earth surface processes because understanding the coevolution of ecosystems and landscapes is one of the grand challenges in earth surface research (NRC, 2010). In that context, we present data over a range of spatial scales that characterize fundamentals of geologic, hydrologic and geochemical controls on the evolution of the important complex of wetland ecosystems that occur within the prairie pothole region (PPR) of North America. The PPR wetlands

belong to a large class that Fan and Miguez-Macho (2011) describe as mostly precipitation and local run-off fed; a class that includes ombrotrophic (rain fed) bogs and nutrient poor fens found worldwide. However, the pothole wetlands have a dramatic range in salinity and composition compared to the mostly fresh water wetlands in this class. Our study emphasizes measurements that quantify the integrated long-term geologic controls on wetland geochemistry in a small but hydrologically relevant subunit of the PPR. We then evaluate data from progressively larger portions of the PPR to determine whether regional controls on wetland water chemistry over the PPR landscape are qualitatively or quantitatively different.

1.1. Prairie pothole region

The PPR spans portions of five states and three Canadian provinces, comprising an area of over 750,000 km² (Fig. 1a), and constitutes one of the largest inland wetland systems on earth (see Fan and Miguez-Macho, 2011). It is named for the mosaic of small (generally <1 ha) pothole-like wetlands that dot the landscape (Fig. 1b). van der Valk

[☆] DISCLAIMER: Any use of trade, firm, or product names is for descriptive purposes only and does not imply endorsement by the U.S. Government.

* Corresponding author. Tel.: +1 303 2361521.

E-mail address: mgold@usgs.gov (M.B. Goldhaber).

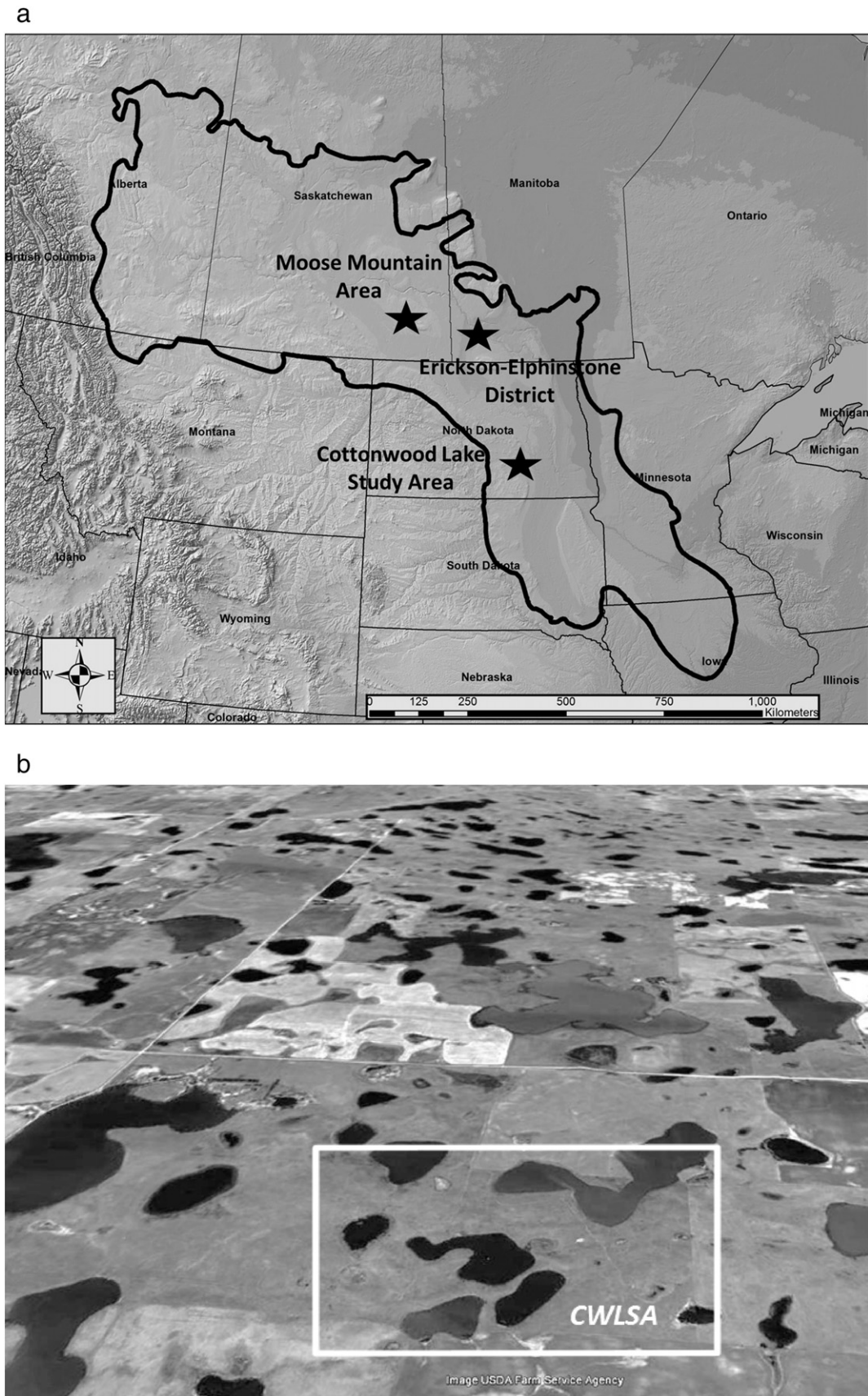


Fig. 1. (a) Outline of the prairie pothole region in the north central US and southern Canada. Stars indicate the locations of the Cottonwood Lake study area (CWLSA), Moose Mountain area, and the Erickson-Elphinstone District as discussed in the text. (b) Google Earth view of the CWLSA and surrounding area in Stutsman County, ND looking north showing the density of wetlands. The box identifies the Cottonwood Lake study area (CWLSA) which is approximately 1.2 km across.

and Pederson (2003) estimated the existence of 12.6 million such wetlands prior to European settlement and Kantrud et al. (1989) estimated that in the 1960s there were 2.3 million wetlands in North and South Dakota with a total area of 1.04 million ha.

The southwestern border of the PPR follows the maximum extent of late Pleistocene glaciers, which traversed North America from northeast to southwest. They shaped the surficial landscape and provided the geologic material that defines the hydrologic and geochemical characteristics of the region (Jones and Deocampo, 2003). Melting of the ice sheet left behind a blanket of heterogeneous and unsorted glacial sediment (i.e. glacial till) resulting in a hummocky topography. The glacial till has low permeability (Lissey, 1971; Freeze and Cherry, 1979; van der Kamp and Hayashi, 2009) causing precipitation to accumulate on the surface in the form of small lakes and ponds. This ponded surface water is subsequently referred to in this paper as wetland water. The wetlands are generally internally drained (note the lack of rivers visible in Fig. 1b), a characteristic that has been termed depression focused flow (Lissey, 1971). When connections between wetlands do occur, they are by a fill and spill mechanism (van der Kamp and Hayashi, 2009). Although the underlying till has low permeability, groundwater hydrology is nonetheless an important determinant of long-term wetland water balance (van der Kamp and Hayashi, 2009) and the chemical composition of wetland water (LaBaugh, 1989).

The till contains reactive minerals including quartz and feldspar from the granitic Canadian Shield, dolomite and calcite from southern Canadian Paleozoic carbonates, and pyrite from late Cretaceous organic rich marine shale that directly underlies portions of the PPR. The Pierre Shale is prevalent as bedrock in North Dakota (Winters, 1963) and its stratigraphic equivalents occur in Canada. Previous studies have shown that weathering of reactive sulfide and carbonate minerals along groundwater flow paths in the till is an important control on the chemical composition of water in PPR wetlands (Rozkowski, 1969; Hendry et al., 1986; Swanson, 1990; Keller et al., 1991; Vanstempvoort et al., 1994; Heagle et al., 2007, 2012; Nachshon et al., 2013). Dissolution of carbonate minerals is a major source of Ca^{2+} and Mg^{2+} ions while pyrite oxidation is the source of SO_4^{2-} to PPR groundwater and wetland water. It is also widely recognized that over both local and regional scales, the chemistry of PPR wetland waters is highly variable in both salinity and solute composition (e.g. LaBaugh, 1989; Last, 1999). Owing to selective removal of Ca-rich carbonate phases, wetland waters generally evolve with increasing salinity towards depletion in Ca^{2+} and enrichment in Na^+ , Mg^{2+} , and SO_4^{2-} (Jones and Deocampo, 2003). With further increases in salinity, SO_4^{2-} -bearing evaporite phases may ultimately precipitate (Last and Ginn, 2005).

In addition to local and regional spatial variability, there are large temporal variations in the chemical composition of individual PPR wetlands due to seasonal, interannual, and decadal changes in water balance. Seasonal variability is controlled by concentration of solutes by evaporation in summer, further concentration by freezing in winter, and dilution during melting of ice and accumulated snowpack in spring. Longer-term climate shifts may lead to episodes of major evaporation or dilution. Wetland chemistry in the PPR therefore reflects a dynamic interplay between climate, topography, groundwater–till interactions, and hydrology (LaBaugh et al., 1996).

A motivation for this study is the close tie between PPR hydrogeochemical processes and biology. There is intense interest in the vertebrate fauna of the PPR for aesthetic and economic reasons. The region is a breeding ground for a large portion (~50%) of all North American waterfowl and has been called ‘the duck factory of North America’ (Eisenlohr, 1967). The floral and invertebrate populations that waterfowl depend on for habitat and food are greatly influenced by wetland salinity and chemical composition (Stewart and Kantrud, 1972; Euliss et al., 1999, 2002, 2004). Thus, geologic, geochemical, hydrologic, climatic, and biological processes all interact to determine habitat suitability for vertebrate fauna (Euliss et al., 2004).

Given its importance as an ecosystem determinant, there is a need to characterize and quantify critical zone processes contributing to the spatial and temporal variability of PPR wetland water chemistry. In this study, we emphasize major controls on the long-term evolution of this system rather than the superimposed annual to decadal variability. We do this at multiple spatial scales beginning with the Cottonwood Lake study area (CWLSA), located about 36 km northwest of Jamestown in Stutsman County, North Dakota, USA. At this site, we use the extensive knowledge of the existing groundwater flow system (Winter, 2003), new and historical groundwater and wetland water chemical data, and inverse geochemical modeling to identify existing geochemical reservoirs and important reactions. We also use chemical and mineralogical analyses from core samples and sulfur isotope compositions of solid and aqueous phases in the system to show that formation of a brown oxidized upper till zone is a proxy for the extent of pyrite oxidation. This allows us to estimate the amount of sulfate generated in the CWLSA and compare this to estimates of SO_4^{2-} stored in various aqueous and solid phase pools.

We next scale up our results by compiling data on the extent of the brown zone in a 9700-km² surrounding area and compare wetland water chemical compositions of this larger area with those of the CWLSA. Finally, we extend the results to the Canadian portion of the PPR by comparing trends in wetland water composition across a broad swath of the North American PPR.

1.2. Cottonwood Lakes study area

The CWLSA is a 92 ha parcel purchased by the US Fish and Wildlife Service in 1963 as a waterfowl production area. Situated near the eastern edge of the Missouri Coteau, the CWLSA occupies an elevated portion of the late Pleistocene glaciated area lying between the Missouri Escarpment and the present day Missouri River. The Coteau consists of a stagnation moraine and glacial outwash sediments (Sloan, 1972). At the time of purchase, 18% of the CWLSA was cultivated farmland and the remainder was native prairie and wetlands. The farmland was subsequently planted in smooth brome and alfalfa. It is underlain by approximately 160 m of glacial till and contains eight seasonally flooded and nine semi-permanently flooded wetlands. The former usually undergo seasonal dry-down (i.e. ponded water disappears in mid-to-late summer; Fig. 2). Research on the flora and fauna has been continuous since 1966 (Swanson et al., 2003) and approximately 55 test holes were drilled in the CWLSA using a power auger to support hydrologic research (Winter and Carr, 1980). This drilling indicated that the till is clayey silt with some large boulders and occasional, potentially-continuous sand layers.

Based on the long-term studies, the dominant water input to wetlands is runoff and direct precipitation to the wetland surface (e.g. Carroll et al., 2005). However, this input does not explain the range of salinity. The salts are introduced by critical zone interactions making weathering and groundwater flow important long-term controls on wetland geochemistry. Groundwater flow is dominated by an upper oxidized and fractured till zone likely ranging from 5 to 15 m thick, termed the effective transmission zone by van der Kamp and Hayashi (2009). Hydraulic conductivities in the effective transmission zone may range from 0.1 to over 1000 m year⁻¹. Deeper till tends to have very low permeability (hydraulic conductivities of 0.001–0.1 m year⁻¹).

Seasonal wetlands, located at local topographic highs (T5, T8, T9; Fig. 2), recharge groundwater. Wetlands at intermediate topographic positions (P3, T2, T3, T4, T6, and T7) are flow-through wetlands that receive and recharge groundwater. Local discharge wetlands are situated in topographically low positions and include semi-permanent wetlands P1, P2, P4, P6, P7, and P8 (Euliss and Mushet, 2011). The total relief is about 33 m. Here we emphasize weathering inputs to discharge wetland P1, because it has been the focus of several previous studies. In addition, other permanent wetlands have more complicated hydrology

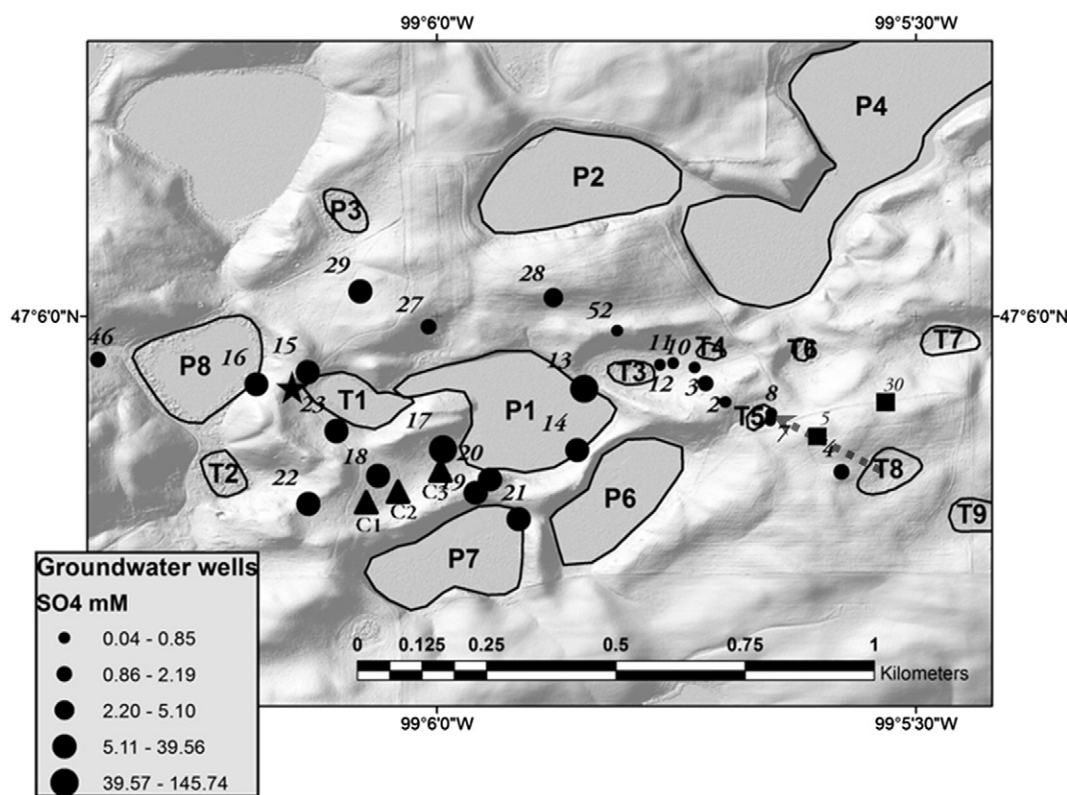


Fig. 2. Lidar image of the Cottonwood Lake study area (CWLSA) with wetlands labeled in large text and groundwater wells indicated by solid circles and small text. The designations T and P were originally for temporary and permanent. For groundwater sites, the size of the circle is proportional to the groundwater SO_4^{2-} concentration measured in samples from the wells. The star indicates the location of the deep test hole and the triangles labeled C1, C2, and C3 indicate the locations of the Geoprobe cores. The dashed line shows the location of a groundwater flow path described in the text.

(P8) or are not entirely on the CWLSA (Winter, 2003). See supplemental material for further description of CWLSA hydrology.

2. Methods

The sampling program was designed to characterize the chemistry of wetland water and groundwater as well as the chemistry and mineralogy of the near surface geologic materials to evaluate how critical zone processes have influenced CWLSA geochemistry. Additional details on methodology are given in Section 2.0 of the supplemental materials.

2.1. Water sampling and analyses

Wetland water was collected on several occasions from July 2009 to September 2011. All CWLSA wetlands that contained water were sampled in July 2009, but only select wetlands were subsequently sampled. Water was collected with a 1.35 m long, 10 cm diameter acrylic tube designed to obtain a representative sample of the water column (Swanson, 1978). For large wetlands, water samples were collected near-shore by wading in to 1 m depth. For shallower wetlands, water samples were taken near the wetland center. Samples were always collected in open water if it existed and care was taken to avoid water containing disturbed sediment material. Samples were temporarily stored in 20 L polypropylene carboys until they were filtered in the field or in the laboratory the same day as collected.

Wetland water pH was measured in-situ except for samples collected in July 2009. For these samples, pH was determined several days after collection and thus was potentially higher than if measured in-situ due to CO_2 degassing. This potential difference in measured pH was tested during three different sampling dates in April and May 2010. Water was collected from five wetlands and pH was measured both in-situ and several hours later. For wetlands T8, T3, P8, and T2, pH in the lab

was up to 0.5 units higher than in-situ. For wetland P1, lab pH was up to 0.2 units lower than in-situ. The reason for this decrease is not clear.

Groundwater was sampled from water table monitoring wells with a peristaltic pump during Aug. 2009 and Aug. 2010. Either a peristaltic pump or a hand operated foot valve pump was used in Sept. 2011. In Aug. 2009, water was pumped from wells until the pH and temperature remained constant, then collected into a 1 L bottle and immediately filtered. In August 2010, several liters of water were purged from wells and the wells were allowed to recover overnight followed by sample collection. The purge water was collected from several wells to assess the influence of different purging schemes on groundwater chemistry. In September 2011, all wells were purged 1 or 2 days prior to groundwater collection.

All samples were filtered using a 0.45 μm pore size Pall Supor® membrane. For July 2009 wetland water samples, subsamples for alkalinity and sulfur isotope analysis of aqueous SO_4^{2-} were not filtered. Subsamples for analysis of cations were preserved with concentrated trace metal grade nitric acid. Samples were stored at 5 °C until analysis.

Cations and anions were analyzed in USGS laboratories using ICP-MS, ICP-AES, and IC as described by Taggart (2002). Alkalinity was determined by Gran titration. See supplemental materials for additional method details.

2.2. Core sampling and analysis

Three cores were drilled in August 2010 to characterize the chemistry and mineralogy of glacial till at the CWLSA and identify features resulting from surface weathering. Cores (5 cm diameter) were obtained with a direct-push, truck-mounted Geoprobe® tool. Cores were collected in plastic liners, capped, and transferred to the lab where they were stored unrefrigerated until processed. The cores were sampled in progression on a slope leading down towards the southwest

edge of wetland P1. Core 1 was collected approximately mid-slope and core 3 was collected near the edge of P1 (Fig. 2). Cores were visually characterized in the laboratory for texture and Munsell color and were divided into depth intervals for further analysis based on visual similarities. Samples were then dried at room temperature, sieved to <2 mm, and ground for chemical and mineralogical analysis (Smith et al., 2009). Clay-rich samples were gently disaggregated using a mortar and pestle prior to sieving.

A set of archived samples from a deep test well drilled to bedrock in 1978 (Winter and Carr, 1980) were also analyzed. These samples had been air dried and stored in cloth bags since the time of collection. The samples were not sieved prior to grinding because they had dried to a dense mass. Therefore, the geochemistry of archived deep test well and more recently collected samples may differ if the composition of coarser material in the former adds a systematic bias to the data. All core samples were chemically analyzed by four-acid digestion (HNO_3 , HCl , HF , HClO_4) followed by ICP-AES and ICP-MS (Briggs, 2002; Briggs and Meier, 2002). SGS Minerals in Toronto, Ontario, Canada performed the analyses. Mineral phases in the core samples were determined using semi-quantitative x-ray diffraction (XRD). Mineral identification was obtained using Material Data Inc. JADE® software and mineral quantification utilized the computer program RockJock (Eberl, 2003).

Two additional extractions were done on a subset of glacial till samples. Water soluble S was extracted from ground till samples (supplemental materials Section 2.4 for additional method details) to determine solid phase gypsum concentrations, assuming that all total S in the leachates was from the dissolution of gypsum and that gypsum dissolution was complete (see Section 3 for further justification of this assumption). Extraction of reduced S from glacial till, assumed to be derived from pyrite, was performed as described by Tuttle et al. (1986) (see supplemental materials Section S 2.5 for additional method details). The reduced S was captured as Ag_2S and used in S isotope analyses.

2.3. Sulfur isotope measurements

Sulfate was precipitated as BaSO_4 from aqueous samples following acidification (3 N HCl) to ~ pH 3.5 and addition of excess 0.5 M BaCl_2 . Precipitates were recovered on 0.45 μm cellulose acetate filters and dried overnight at 60 °C. The stable sulfur isotopic composition ($\delta^{34}\text{S}$) of BaSO_4 and Ag_2S precipitates (as prepared above) was determined by isotope ratio mass spectrometry. Samples were transferred to 5 × 9 mm tin capsules, amended with ~2 mg of V_2O_5 , and combusted in an elemental analyzer (Thermo Flash®) interfaced to a mass spectrometer (Thermo Delta Plus XP®) operated in continuous flow mode (Giesemann et al., 1994). Results are reported in delta (δ) notation in parts-per-thousand (‰) deviation relative to a monitoring gas according to;

$$\delta^{34}\text{S} = \left[\left(\frac{R_{\text{sample}}}{R_{\text{standard}}} \right) - 1 \right] * 1000 \quad (1)$$

where $R = {}^{34}\text{S}/{}^{32}\text{S}$ in the sample and standard (see supplemental materials Section 2.6 for additional method details).

2.4. Mineral saturation calculations

Saturation state of carbonate and sulfate-bearing minerals was calculated using Geochemist's Workbench (Bethke, 2008) and thermodynamic data from the Los Alamos National Lab V8 R6 dataset modified for compatibility with Workbench. An extended (b-dot) Debye–Huckel algorithm was used to calculate activity coefficients. We added thermodynamic data for $\text{Mg}_{0.15}\text{Ca}_{0.85}\text{CO}_3$ (Bischoff et al., 1987) because high magnesium calcite is known to precipitate in environments with Mg/Ca ratios of ~2 (Muller et al., 1972), which have been observed for the

more saline wetlands at CWLSA. Mg-rich calcite has been recognized in Canadian PPR wetlands (Last and Ginn, 2005; Heagle et al., 2007).

3. Results

3.1. Wetland water chemistry

The full wetland water chemistry data set is in Table S1 and is plotted in Figs. 3 and 4. The chemistry of individual CWLSA wetland waters varied during our 3-year sampling period due to seasonal and annual cycles of precipitation and evaporation (LaBaugh et al., 1996). However, this seasonal variability was less than the differences in water chemistries between wetlands in this small study area. For example, TDS in wetlands T5 and P1 varied at 27% and 16%, respectively, over the course of the 3-year sampling period. In comparison, the average TDS in wetland P1 water (2740 mg kg^{-1}) was 20 times greater than in T5 (132 mg kg^{-1}). Wetlands at elevations greater than 560 msl and classified as recharge wetlands (T5, T8, and T9) had TDS <200 mg kg^{-1} whereas flow-through and discharge wetlands at lower elevation all approached or exceeded 1000 mg kg^{-1} . Wetland water pH ranged from 6.6 to 7.4 for recharge wetlands, from 7.2 to 8.0 for flow-through wetlands, and from 7.7 to 9.0 for discharge wetlands.

The anion composition of CWLSA wetland waters varied systematically from HCO_3^- dominant at low TDS to SO_4^{2-} dominant at higher TDS (Figs. 3 and 4). Chloride was a minor constituent (Fig. 3). Water in upland recharge wetlands with low TDS had over 90% of the anionic charge attributed to HCO_3^- and was similar to rainwater in anionic ratio (Fig. 4). At the other extreme, SO_4^{2-} accounted for over 85% of the anionic charge in discharge semi-permanent wetland P1 water. Cation compositions of wetland water evolved progressively from Ca^{2+} rich (with subordinate Mg^{2+}) to Mg^{2+} dominant (with an approximately constant proportion of $\text{Na}^+ + \text{K}^+$) with increasing TDS. Therefore, for the period 2009–2011, upland wetlands T5, T8, and T9 were classified as $\text{Ca}^{2+}\text{--HCO}_3^-$ water, whereas discharge wetlands P1 and P8 were $\text{Mg}^{2+}\text{--SO}_4^{2-}$ water. Notably, these wetlands with very different water chemistry are in close proximity (~200 m).

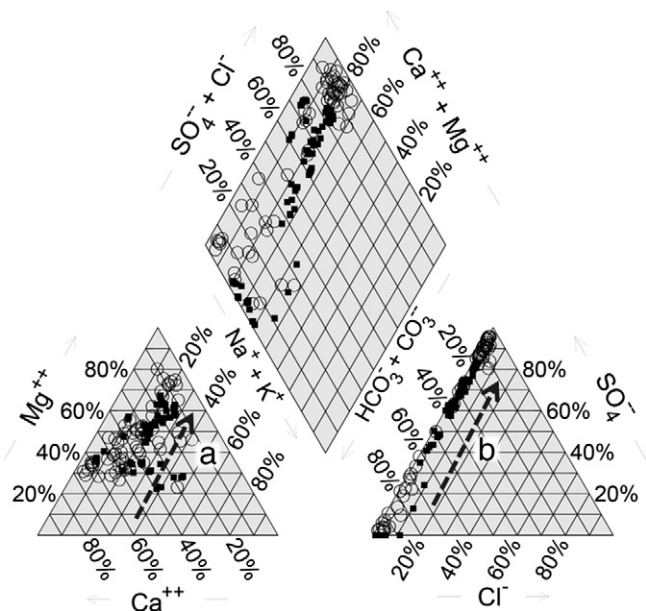


Fig. 3. Piper diagram of groundwater (open circles) and wetland water (closed squares) samples from the CWLSA reported in this study. Note that on the anion triangle at the lower right both groundwater and wetland analysis fall along the $\text{SO}_4^{2-}\text{--HCO}_3^-$ axis of the diagram. The two arrows show the trend in composition with increasing dissolved solids for cations (arrow A) and anions (arrow B).

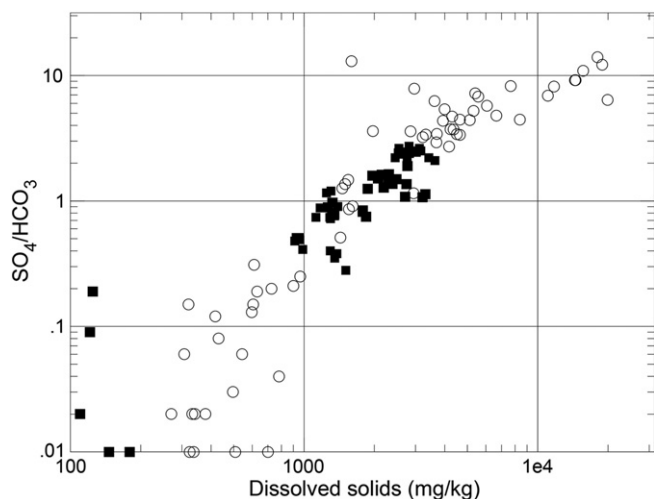


Fig. 4. Plot of the molar ratio of SO_4^{2-} to HCO_3^- in CWLSA water samples versus total dissolved solids (TDS). Wetlands (filled squares) plot in two distinct groupings. Low TDS values are from recharge wetlands, whereas those with higher TDS (>800 mg/kg) are flow through or discharge wetlands. Groundwater samples (open circles) display evolution in the ratio over a broad range of salt content including values greater than those in wetlands.

3.2. Groundwater chemistry

Table S2 contains the full chemical data set for groundwater and includes data from Swanson (1990) for some of the same wells sampled during this study to permit evaluation of longer-term trends. The data obtained in the 1980s by Swanson represent a period of mild dry conditions (Winter and Rosenberry, 1998) compared to historically very wet conditions over the period of our sampling. Despite this climatic difference, the chemical data show relatively small temporal differences for individual wells compared to the large differences observed among wells. The exceptions were wells 13 and 15 which are located at the edge of wetland P1, an area of particularly dynamic hydrogeochemistry (Arndt and Richardson, 1993; Rosenberry and Winter, 1997; Mills et al., 2011).

The TDS trend in groundwater wells mirrored that of wetland waters with upland wells (e.g. wells 2, 4, 7, 10, 11, and 12) less saline than those in lower-lying areas (e.g. wells 13, 15, 17, 18, 21, 22, and 27). Two exceptions were upland wells 5 and 30 which were compositionally similar to wells in low-lying areas. These wells may access a hydrologically-isolated pocket of water that has had a very long time to interact with till. The pH of groundwater ranged from 6.9 to 9.0, but was typically near neutral for most wells. Groundwater cation and anion compositions both followed the same trend with increasing TDS as observed for wetland waters (Fig. 4). However, water from several wells had higher TDS (up to 19 g L^{-1}) and SO_4^{2-} concentrations (up to 140 mM) than discharge wetlands. Specifically, wells adjacent to wetland P1 (13, 17, 18, 19, 20, 25) had higher TDS and SO_4^{2-} concentration than wetland P1 water. These adjacent wells also had lower pH and larger $\text{Ca}^{2+}:\text{SO}_4^{2-}$ ratios than P1 water.

3.3. Mineral saturation

From wetland and groundwater chemistry it is apparent that calcium carbonates and gypsum are important solid-phase buffers of PPR hydrogeochemistry. The saturation states of gypsum and high-Mg calcite are plotted in Fig. 5. Water in upland recharge wetlands T5, T8, and T9 is undersaturated with respect to both high-Mg calcite (as well as low-Mg calcite) and gypsum. Flow-through and discharge wetlands are either supersaturated or approximately saturated with high-Mg calcite. Samples from 2009 for which the pH was measured post-filtration (and may have outgassed) are not systematically more supersaturated than those with in situ pH data. Dolomite (data not

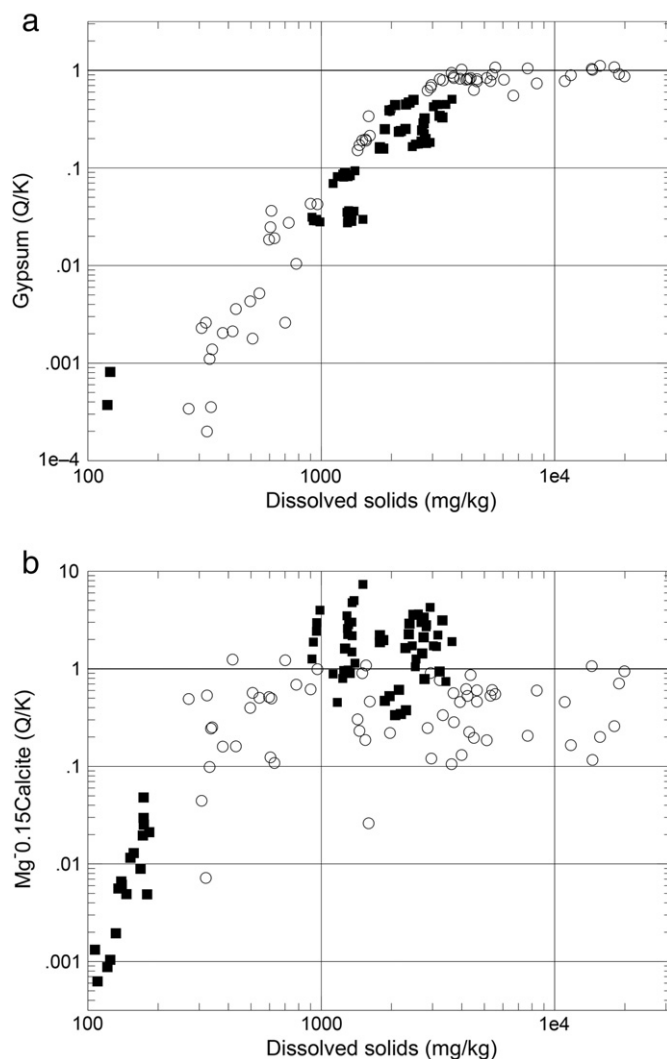


Fig. 5. Log-log plot of saturation state of gypsum (Fig. 5a) and Mg-rich calcite (Fig. 5b) versus total dissolved solids in CWLSA wetland water and groundwater samples. Q/K is the saturation state of the mineral, defined as the ratio of the ion product divided by the solubility product at saturation. Values less than 1 indicate undersaturation, values greater than 1 indicate supersaturation. Wetlands (filled squares) are undersaturated with gypsum but may be undersaturated saturated and even supersaturated with Mg-rich calcite. Groundwater samples (open circles) range from undersaturated to saturated for both solid phases; most are undersaturated with carbonate but many of the groundwater samples are saturated with gypsum ($Q/K \sim 1$).

plotted) is undersaturated from upland wetlands and a subset of upland groundwater wells but is supersaturated in most other water samples. Groundwater samples were generally undersaturated with high-Mg calcite and calcite. Two groundwater analyses at or above saturation were from well 12, which is in wetland (T3) that had ponded water supersaturated with high-Mg calcite. Another saturated sample was from well 13 located at the edge of wetland P1 (discussed elsewhere). All wetland waters were undersaturated in gypsum but water from some wells surrounding wetland P1 (13, 17, 20, 61, and 18) were saturated. Both B-dot and Harvey Moller activity coefficient models produced similar results for the saturation state of gypsum. Mineral saturation trends similar to those in Fig. 5 have been previously reported from wetlands in Nelson County, ND (Arndt and Richardson, 1989).

3.4. Core chemistry and mineralogy

Chemical and mineralogical data for selected solid samples from cores 1, 2, and 3 and the archived samples from the deep well drilled

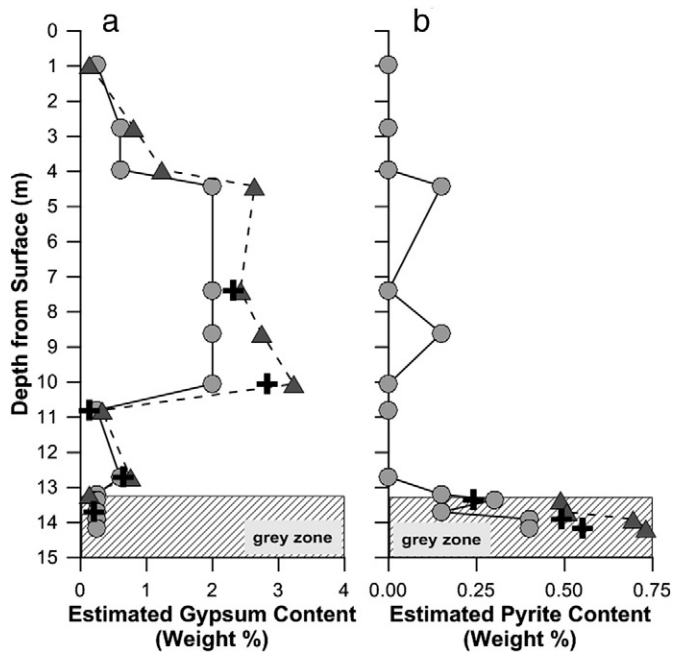


Fig. 6. Depth profiles of estimated (a) gypsum and (b) pyrite content of select glacial till samples from core 1. Three different estimates are plotted: XRD (circles), calculated from total S (triangles), measured from water leaches (gypsum) or reductive dissolution (pyrite) (crosses). For samples that had XRD gypsum concentrations of <0.5 wt.%, points are plotted at values of 0.25 wt.%. For samples that had XRD pyrite concentrations of <0.3 wt.%, points are plotted at values of 0.15 wt.%. For samples that had no detectable pyrite by XRD, points are plotted at values of 0.00 wt.%. Gypsum and pyrite estimates from total S concentrations assume all S in the brown zone is present in gypsum and all S in the gray zone is present in pyrite. The indicated gray zone was determined by visual observations of till color.

in 1978 are presented in Table S3. Select data from core 1 are plotted in Fig. 6. Cores 1, 2, and 3 penetrated to depths of 14.3, 10.1, and 7.8 m, respectively. The deep well was drilled to a depth of 136.4 m and penetrated the Pierre Shale at 135.6 m. A brown–gray color transition was observed at 13.3, 7.34, and ~ 10 m for cores 1 and 3 and the deep test well, respectively. The transition was not penetrated by core 2. This color transition has been observed elsewhere in the PPR (see Section 3.6 below). The brown zone material from cores 1 and 3 was visually similar: silty clay texture with occasional veins and nodules of Fe and Mn oxides, lithic fragments, and white crystals that are identified as gypsum and calcite based on the presence of these phases in XRD spectra. Material from the gray zones of cores 1 and 3 was dark gray with lithic fragments. The material from the test well was not visually characterized in detail.

The XRD data indicate that all core samples contained potassium and plagioclase feldspar (5–7 wt.% and 8–13 wt.%, respectively), calcite (5–9 wt.%), dolomite (7–9 wt.%), silica in the form of opal (4–12 wt.%), amphibole (2–3 wt.%), quartz (27–38 wt.%) and the clay minerals smectite (3–8 wt.%), illite (7–14 wt.%), and chlorite (4–7 wt.%) (Table S3). All core samples, except the shale bedrock from the deep well, had similar concentrations of total inorganic carbon (average 1.9 ± 0.2 wt.% C; 1σ), which were consistent with calcite and dolomite content determined by XRD (13 ± 2 combined wt.%). The average organic carbon content of brown zone samples (0.28 ± 0.14 wt.%; 1σ) was lower than that of gray zone samples (0.52 ± 0.11 wt.%). These averages do not include values for near-surface samples (<1.5 m) in the brown zone or the shale sample in the gray zone. Organic carbon depletion in oxidized till has been reported by Keller et al. (1991) and attributed to oxidation by atmospheric oxygen.

Pyrite was detected by XRD at ≥ 0.3 wt.% in gray zone samples but was <0.3 wt.% or not detected in samples from the brown zone (Table S3). Pyrite estimated by reductive dissolution for select gray

zone samples was generally greater than, but was positively correlated with, pyrite concentrations by XRD (Fig. S1a). Total S concentrations in gray zone samples were moderately correlated with pyrite by XRD (Fig. S1a). The depth distribution of estimated pyrite concentration in core 1 samples is plotted in Fig. 6(b).

Gypsum was frequently detected by XRD in brown oxidized sediments but was below quantifiable concentration (<0.5 wt.%) in all gray zone samples and some brown zone samples (Table S3). Gypsum was present at concentrations between 1 and 8 wt.% in about half of the brown zone samples. Gypsum concentrations estimated by leaching select core samples with water and measuring dissolved SO_4^{2-} were well-correlated both with gypsum concentrations determined by XRD and gypsum concentrations estimated by total S concentrations (Fig. S1b). The depth distribution of estimated gypsum content in core 1 is plotted in Fig. 6(a). Gypsum has previously been recognized in CWLSA upland sediments (Swanson, 1990).

3.5. Sulfur isotopes

The $\delta^{34}\text{S}$ values of sulfate ($\delta^{34}\text{S}_{\text{sulfate}}$) in wetland water, groundwater, and gypsum from core samples as well as $\delta^{34}\text{S}$ values of pyrite ($\delta^{34}\text{S}_{\text{pyrite}}$) from core samples ranged from -22.1% to $+1.7\%$ (Tables S1–S3, Fig. 7). With the exception of dissolved SO_4^{2-} in a few wetland samples, the majority of both aqueous and solid phase samples had negative $\delta^{34}\text{S}$ values. Although the range in wetland water $\delta^{34}\text{S}_{\text{sulfate}}$ values was rather large (-16.9% to $+1.7\%$), there was a distinct bias towards more positive $\delta^{34}\text{S}_{\text{sulfate}}$ values in wetland water (mean value -5.0%) compared to groundwater (mean -10.6%). Both wetland water and groundwater were more positive than gypsum (mean

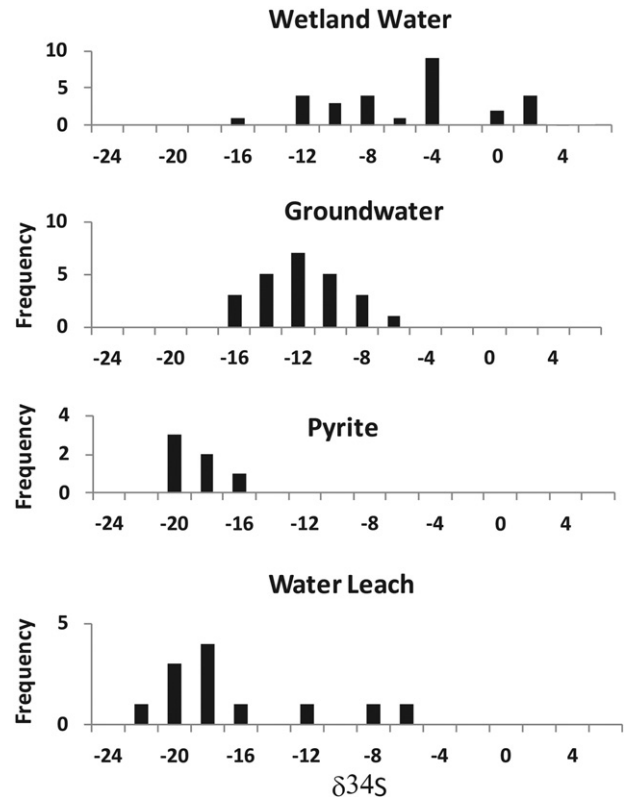


Fig. 7. Histograms of the $\delta^{34}\text{S}$ values of sulfate in wetland water, groundwater and water leach samples (water leach values are equivalent to solid phase gypsum) as well as reduced sulfur in pyrite in the CWLSA. Similar values for $\delta^{34}\text{S}$ values for pyrite and gypsum in the till provide evidence that oxidation of pyrite is the ultimate source of most sulfate in this system. Progressively less negative $\delta^{34}\text{S}$ values for SO_4^{2-} dissolved in groundwater and wetland water may indicate removal of isotopically light sulfur by microbial sulfate reduction.

–16.5‰) and pyrite (mean –19.9‰) in till. The single analysis of pyrite from the Pierre Shale at the base of the deep test hole had a $\delta^{34}\text{S}$ value of –16.5‰.

There is a positive correlation between $\delta^{34}\text{S}_{\text{sulfate}}$ and pH for wetland water and groundwater samples (Fig. 8a). Groundwater samples group at lower pH and $\delta^{34}\text{S}$ values and have little overlap with wetland waters. The $\delta^{34}\text{S}_{\text{sulfate}}$ values from wetland P1 water samples were more positive than $\delta^{34}\text{S}_{\text{sulfate}}$ values from immediately adjacent groundwater wells 13, 18, 23 and 61. There is also a tendency for those groundwater and wetland water samples that are at or very near saturation with gypsum to have more negative $\delta^{34}\text{S}$ values (Fig. 8b). The isotopic composition of these gypsum saturated waters in fact overlap with the $\delta^{34}\text{S}_{\text{gypsum}}$ values in core samples, which is consistent with both chemical and isotopic equilibrium between coexisting solid and aqueous SO_4^{2-} .

3.6. Thickness of the Upper Brown Zone in the CWLSA

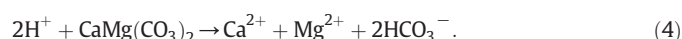
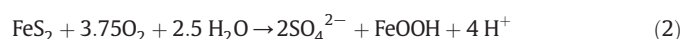
The presence of a transition within the critical zone from an upper brown zone to an underlying gray zone is a feature recognized throughout the CWLSA as has been reported elsewhere in the PPR (e.g. Hendry et al., 1986; Keller et al., 1989, 1991). Drilling logs that note the depth of this color transition were obtained for nearly all groundwater-

monitoring wells (T. Winter, written communication, 2010). The depth of this transition was interpolated throughout the CWLSA area using a spline algorithm in ArcGIS® to create a contour plot (Fig. 9). The outline of individual wetlands was added as a barrier to the contour effectively treating wetlands as having no upper brown zone. This seemed appropriate given the organic-rich reducing character of wetland sediments (see also Heagle et al., 2012), which we believe precludes formation of oxidized sediments.

4. Discussion

4.1. Evolution of wetland and groundwater chemistry

A characteristic of wetland water geochemistry in the CWLSA is the remarkable variability in salinity and ionic composition at spatial scales <0.5 km. As has been shown previously (Wallick, 1981; Van Stempvoort et al., 1994; van der Kamp and Hayashi, 1998, 2009), we explain this variability by oxidation of pyrite in the till summarized by the reactions:



Oxidation of pyrite forms SO_4^{2-} and produces protons that drive dissolution of dolomite and calcite. The products of these coupled reactions are solid phase iron oxy-hydroxides and aqueous SO_4^{2-} , Mg^{2+} , Ca^{2+} , and HCO_3^- . The ions migrate down hydrologic gradients from higher topographic positions and accumulate in local topographic depressions or form gypsum (Arndt and Richardson, 1993).

Two lines of evidence support pyrite oxidation as the primary driver for PPR hydrochemistry. First, mineralogical and geochemical data demonstrate that the upper several meters of the till has been oxidized. The contrast between the upper brown zone and the gray material below indicates the presence of brown Fe(III)-bearing oxides in the surface material. Our data (Table S3; Fig. 6) demonstrate that the unoxidized till contains pyrite but the overlying brown till does not. The solid phase host for sulfur in the brown zone is largely gypsum. Second, the predominantly negative isotopic composition of sulfur in the CWLSA indicates a shale-derived pyrite source. The range of $\delta^{34}\text{S}$ values that we determined for pyrite in the CWLSA gray till and bedrock (–16.5 to –21.7‰) is typical of pyrite sources from marine shale (Goldhaber, 2004) and similar to the mean $\delta^{34}\text{S}$ value of –18.5‰ determined for pyrite in the midcontinent Cretaceous marine shale, the source of shale in the PPR (Gautier, 1987; Whittaker and Kyser, 1990). Because negligible isotopic fractionation is associated with S oxidation and gypsum precipitation (Ohmoto and Goldhaber, 1997), the negative $\delta^{34}\text{S}$ values and both solid phase and aqueous sulfate are direct evidence that marine pyrite is the source for this very S-rich, terrestrial environment. More positive $\delta^{34}\text{S}_{\text{sulfate}}$ values for some groundwaters and several wetland waters are attributed to isotopic fractionation during microbial sulfate reduction.

4.2. Fluid evolution along a groundwater flow path

We used inverse geochemical modeling (NetPathXL; <http://pubs.usgs.gov/tm/06A26/>) to illustrate that oxidation of pyrite and dissolution of carbonates over time can account for the current variability in the chemical composition of groundwater along a hydrological flow path in the CWLSA. The flow path modeled started with recharging fluids from wetland T8 and ended at well 7 located ~150 m downslope (Fig. 2). We assumed that groundwater migrating towards well 7 is a

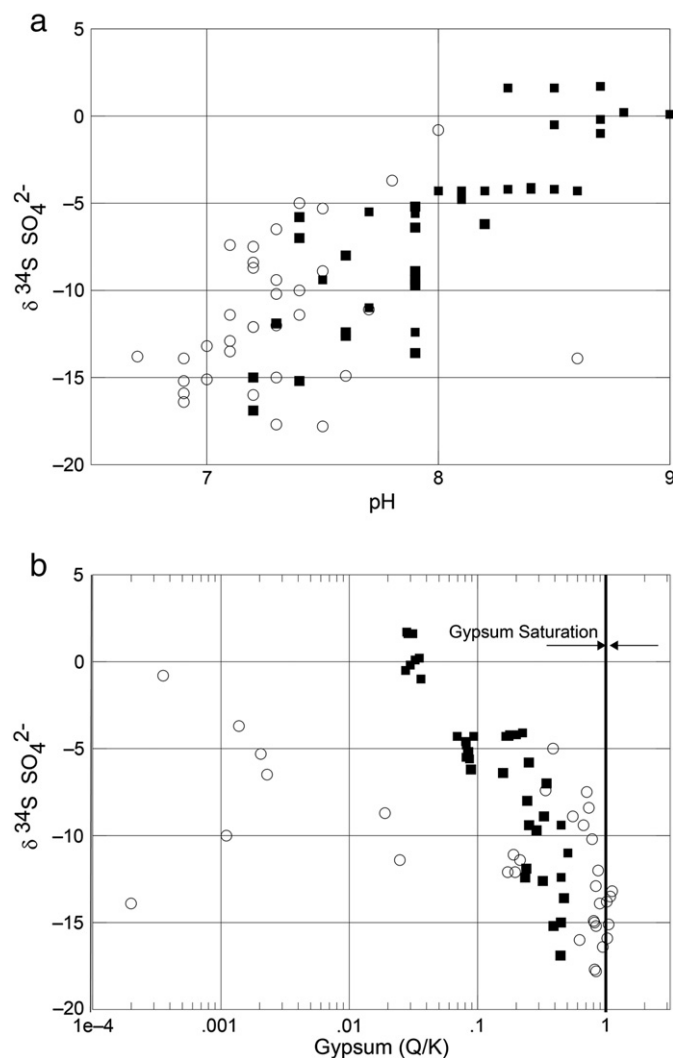


Fig. 8. Plots of $\delta^{34}\text{S}$ values for dissolved SO_4^{2-} in CWLSA water samples vs. (a) pH and (b) saturation state of gypsum. Open circles are groundwater, filled squares are wetland water. Groundwater samples at or near saturation with gypsum (i.e. Q/K values \sim 1) have more negative $\delta^{34}\text{S}_{\text{sulfate}}$ values.

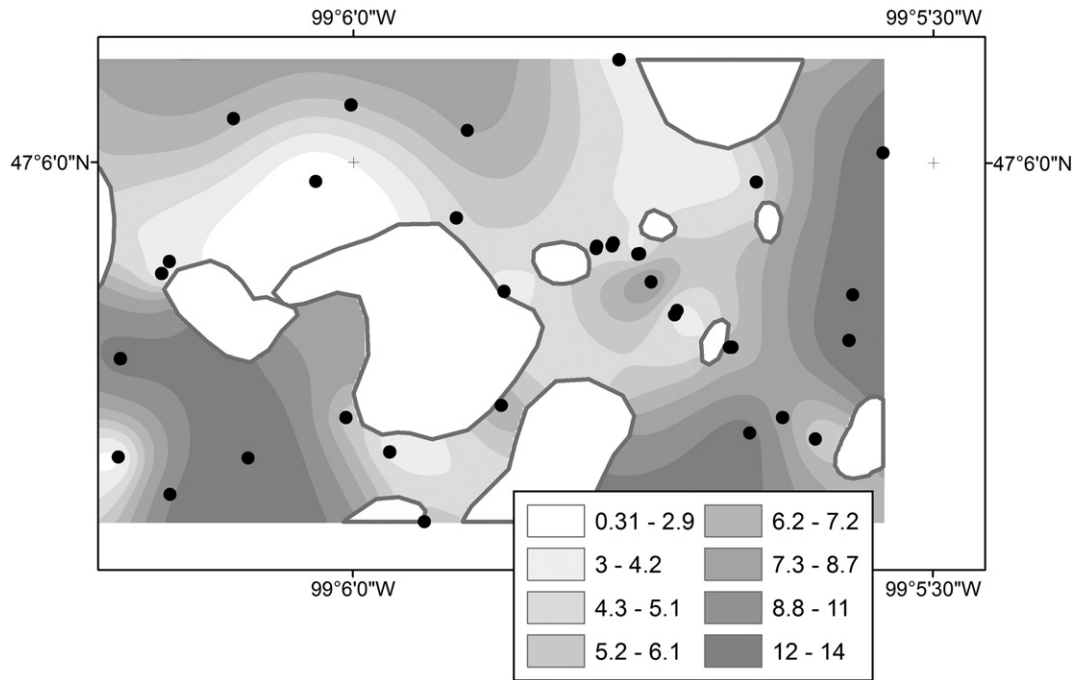


Fig. 9. Contour plot of the thickness of the brown oxidized zone in the CWLSA. The legend is the contoured thickness in meters and black dots are control points. The area shown in this figure does not match Fig. 2 because we limited the calculation to that portion of the study area with well logs documenting brown zone thickness. The wetlands are assumed to lack a brown zone below them due to reducing conditions in the sediments.

mixture of surface water recharging from wetland T8 and winter precipitation (LaBaugh et al., 1998). The data used for the chemical composition of winter precipitation were from the National Atmospheric Deposition Program's site ND11 located 12.6 km NW of the CWLSA and represent a weighted mean from winter 2008 to 2009. The mixing ratio of these two fluids was constrained by unpublished data ($\delta^{18}\text{O}_{\text{H}_2\text{O}} = -10.0\text{‰}$, -20.0‰ , and -11.7‰ for wetland T8, precipitation, and well 7 respectively). Additional constraints on the system were initial and final concentrations of Na^+ , Ca^{2+} , Mg^{2+} , SO_4^{2-} , and HCO_3^- (data from Tables S1 and S2).

Calcite, dolomite, and pyrite, identified in this study by XRD, were chosen as reactive phases initially present in the till. The carbonate phases are likely present throughout the till section (see e.g. Table S3). Pyrite may be available to migrating fluids as a residual phase in the oxidized portion of the flow path or concentrated in the basal region of the oxidized zone (e.g. Fig. 6). Lignite having an average composition of $\text{CH}_{0.8}\text{O}_{0.2}$ was selected as a potential source of oxidizable organic matter. Lignite has been recognized in the till by Winters (1963) and our organic carbon measurements suggest less organic carbon in the brown versus gray zone material. Both ion exchange on clay minerals and redox transformations were accommodated by the modeling code.

The results of the net mass balance calculations returned from this model were not unique. However, using knowledge of aqueous and solid phase geochemistry (Plummer et al., 1983) the most plausible results were selected. Model results that required precipitation of calcite or dolomite were rejected because these phases are undersaturated in upland groundwater. A plausible model along the flow path involves dissolution of 0.1 mmol L^{-1} of calcite and 0.84 mmol L^{-1} dolomite, oxidation of 0.09 mmol L^{-1} pyrite, loss of 0.37 mmol L^{-1} CO_2 , and addition of 0.01 mmol L^{-1} O_2 . Lignite oxidation was not required for mass balance. Overall, the model predicts trends that are in general agreement with reactions summarized in Eqs. (2)–(4). Thus, present day upland geochemical processes supply Ca^{2+} , Mg^{2+} , SO_4^{2-} , and HCO_3^- to the groundwater flow system converging on wetland P1.

4.3. Evolution of groundwater to wetland water

Comparison of aqueous chemical data for discharge wetland P1 with adjacent groundwater samples from wells 18, 20, 23, 25, and 26, reveal consistent differences. Compared to adjacent groundwater, P1 water is systematically depleted in Ca^{2+} , Mg^{2+} , and SO_4^{2-} and enriched in Na^+ , Cl^- , and HCO_3^- . The wetland water also has a higher pH and more positive $\delta^{34}\text{S}_{\text{sulfate}}$ values. These differences suggest that, if groundwater is a significant input to the wetland, then internal wetland processes modify those inputs. Inverse geochemical modeling was used to characterize the net processes responsible for the observed compositional shifts. For these calculations, water sampled from well 23 was chosen as the starting fluid and water from wetland P1 as the ending composition (data in Tables S1 and S2). This analysis assumes that the dominant fluid flow path is by groundwater flow rather than surface flow. Addition of surface runoff would dilute wetland water and lead to the same general conclusions, but with a larger role for evaporation. Based on the mass balance modeling of Carroll et al. (2005) for wetland P1 and the chemical compositions of groundwater and rainwater discussed in this paper, we calculate that groundwater accounts for over 95% of the total input of SO_4^{2-} into wetland P1 on an annual basis. The reactive mineral phases for this calculation were the same as for the previous calculation (Section 4.2) with the addition of gypsum based on its abundance in the till surrounding wetland P1. In addition, evaporation was incorporated into the calculation (e.g. Rosenberry et al., 2004).

Model results point to a net precipitation of 13.8 mmol L^{-1} of high-Mg carbonate ($\text{Mg}_{0.15}\text{Ca}_{0.85}\text{CO}_3$) as the driver for Ca^{2+} depletion from 15.2 to 3.2 mM and the smaller decrease in Mg^{2+} from 15.3 to 13.6 mM. Carbonate precipitation is permissible given the fact that wetland waters are saturated or supersaturated with carbonate phases (Fig. 5). Net sulfate reduction (Eq. (5)) occurring in the sediments leading to sedimentary pyrite formation (or solid reduced organic S compounds) is a plausible mechanism for the SO_4^{2-} decrease from 28.5 to 20.1 mM. Pyrite, reduced organic sulfur compounds, and dissolved H_2S are present in wetland P1 sediments (Zeng et al., 2013).

Preferential removal of isotopically light sulfur to the solid phase, leaving residual SO_4^{2-} enriched in the heavy isotope is well documented (Goldhaber, 2004) and is consistent with the increase in $\delta^{34}\text{S}_{\text{sulfate}}$ from -15.9% in the groundwater to -4.3% in the wetland water. Our calculation assumed a net fractionation factor of 15% between SO_4^{2-} and pyrite. Net loss of gaseous isotopically light H_2S from the system would have a similar isotopic effect on $\delta^{34}\text{S}_{\text{sulfate}}$ in the wetland. Sulfate reduction also likely contributes to the observed increase in HCO_3^- from 5.3 mM in well 23 to 6.5 mM in P1 (Eq. (5));



where, CH_2O represents generalized organic matter that is abundant in CWLSA sediments.

Evaporation is predicted by the model and is required for Cl^- to increase from 0.38 mM in well 23 to 0.53 mM in P1. The pH increase is likely attributable to a combination of processes; however, a predicted net loss of 17 mM of CO_2 from the system certainly contributes to this increase. Net carbonate mineral precipitation as a driving mechanism for CO_2 loss from lakes has been previously documented (Stets et al., 2009). The positive correlation between pH increase and $\delta^{34}\text{S}$ increase (Fig. 8a) in wetlands may be related to CO_2 loss (pH increase) that is in turn driven by the linkage between SO_4^{2-} reduction ($\delta^{34}\text{S}$ increase) resulting in bicarbonate generation and carbonate mineral precipitation. The coupling between carbonate precipitation and CO_2 evasion from wetlands has potential implications for the net carbon balance of PPR wetlands.

Based on the inverse modeling, dynamic geochemical processes within the wetland drive the consistent compositional distinction between wetland P1 water, the local groundwater discharge point for the CWLSA, and surrounding groundwater. The most conspicuous indicators of these processes are removal of Ca^{2+} , and to a lesser extent, Mg^{2+} , coupled with less dramatic removal of SO_4^{2-} , increase in $\delta^{34}\text{S}$ of SO_4^{2-} , and increase in pH.

Taken together, the inverse modeling calculations indicate that upland geochemical processes transport key reactive constituents derived from till alteration towards the groundwater reservoir in topographically low portions of the CWLSA. The calculation characterizes a flow path with a transit time that may be measured in hundreds of years and thus, is unlikely to reflect short-term reactions. Internal wetland processes transform these accumulated groundwater constituents to the wetland water compositions that are important determinants of the distribution wetland biota.

4.4. Cumulative effect of near-surface pyrite oxidation on CWLSA water

The map of brown zone thickness for the CWLSA based on well log and core data (Fig. 9) allows us to estimate the total mass of pyrite oxidized to SO_4^{2-} over the entire history of till weathering. A brown zone volume of 2.7×10^6 m³ at CWLSA was calculated using the contoured thickness and the zonal statistics functions in ArcGIS®. This is a minimum estimate because a subset of the upland portion of the CWLSA was not modeled due to lack of drill-hole data. We also assumed no oxidized zone under the wetlands (Section 3.6), although it has been documented elsewhere (Berthold et al., 2004). The total area modeled was 54 ha of the 92 ha that comprise the total CWLSA. Data from cores 1 and 3 and the deep test hole document a pyrite content of the gray zone material of 0.2 – 0.6 wt.%. Assuming that pyrite oxidation within the brown zone is complete, glacial till bulk density is 2.0 g cm⁻³, and an initial (pre-oxidation) pyrite content of 0.3 wt.% (the approximate average gray zone value), we estimate that 1.6×10^{10} g of pyrite have been oxidized in the CWLSA brown zone. Heagle et al. (2012) presented a similar calculation based on a generalized altered zone without the benefit of detailed solid phase oxidized zone constraints.

The estimated pyrite removal corresponds to approximately 1.3×10^{10} g of SO_4^{2-} produced. For comparison, the amount of SO_4^{2-}

dissolved in P1 wetland water in 2009 was only $\sim 6 \times 10^6$ g. Clearly, even if all of the wetlands in the CWLSA are considered, dissolved SO_4^{2-} in wetland water represents a minor fraction of all SO_4^{2-} produced over time in the CWLSA. Other fates for the SO_4^{2-} could be as dissolved SO_4^{2-} in groundwater, as solid phase gypsum, reduction of SO_4^{2-} to form iron sulfides in wetland sediments, or transport of dissolved SO_4^{2-} to the deeper groundwater flow system.

While all of these sinks, particularly loss to deeper groundwater flow, likely account for some of the SO_4^{2-} mass balance in the CWLSA, our data suggest that most of the total SO_4^{2-} produced by pyrite oxidation is stored as solid phase gypsum and/or dissolved sulfate in groundwater. Both XRD and water leach data suggest a ≥ 6 m vertical interval of brown oxidized till that contains ≥ 2 wt.% gypsum in cores 1–3. This interval extends well beyond the present margin of the wetland to the slopes above it. We assume that this gypsum-rich interval occurs in a ring around wetland P1 that is ≥ 100 m in width (core 1 was collected ~ 100 m from the current edge of wetland P1) and we use a diameter of 250 m for P1. We estimate that gypsum in this volume of till could store a minimum of 1.5×10^{10} g of sulfate which accounts for all SO_4^{2-} produced by pyrite oxidation in the CWLSA till. It is also likely that sediments underlying at least a portion of the current open water portion of wetland P1 contain gypsum (C. Mills, unpublished data) making our estimate of total solid phase gypsum a minimum (see also Heagle et al., 2012). This process of progressive SO_4^{2-} accumulation is superimposed upon the many weather-related, and longer-term climate related shifts in the composition of individual wetland waters. Because a large volume of groundwater, whose geochemistry evidently does not change dramatically with time, surrounds wetland P1, it is likely that even significant shifts in wetland water geochemistry will be ultimately buffered by equilibration with the larger groundwater-solute reservoir.

4.5. Scaling up from CWLSA to regional and sub-continental areas

4.5.1. Regional comparison in North Dakota

To evaluate whether the hydrogeochemical processes operating within the CWLSA are representative of larger portions of the PPR, we compared our geochemical data with regional studies. Geochemical data from 178 wetlands in Stutsman and adjacent Kidder counties (an area of ~ 9700 km² that includes the CWLSA-locations in Fig. 10a) collected over the period 1966–1976 (Swanson et al., 1988) are shown in Fig. 11 (see also Fig. S2 in the supplemental materials). There is a clear similarity in trends diagnostic of major geochemical processes between this data and our data for CWLSA wetlands. One contrast with the CWLSA is that Na^+ is a dominant cation for many of the wetlands analyzed on the more regional-scale (Fig. 11b). With increasing TDS, concentrations of Ca^{2+} and then Mg^{2+} decrease relative to Na^+ (plot not shown). This trend towards relatively elevated Na^+ is likely an extrapolation of the trends recognized in the CWLSA driven by preferential removal of Ca^{2+} and Mg^{2+} from wetland waters to solid phase carbonate minerals (a majority of the wetlands sampled by Swanson et al., 1988 were saturated in carbonate minerals). We cannot, however, exclude the possibility of the formation of Mg-rich clays as a sink for this element (Jones and Decampo, 2003) and/or input of NaCl rich fluids from deeper aquifers. Chloride is also more abundant on a relative basis in the regional data set than the CWLSA and the anion composition of a subset of the samples is dominated by this element (Fig. 11a). Some of these Cl^- -rich wetlands may be explained by their proximity to the interstate highway and their susceptibility to input of deicing salts. For others, road salt inputs do not seem likely.

Despite these differences, there is a very important similarity between the regional and CWLSA data sets. They both follow the same trend of anion evolution from HCO_3^- to SO_4^{2-} dominant with increasing TDS (Figs. 11a and S2). This anion trend in the regional data extends beyond that for CWLSA in that the SO_4^{2-} concentrations (and TDS) in many of the wetland waters in the Swanson et al. (1988) data set exceed those measured at CWLSA. This suggests that when expressed over

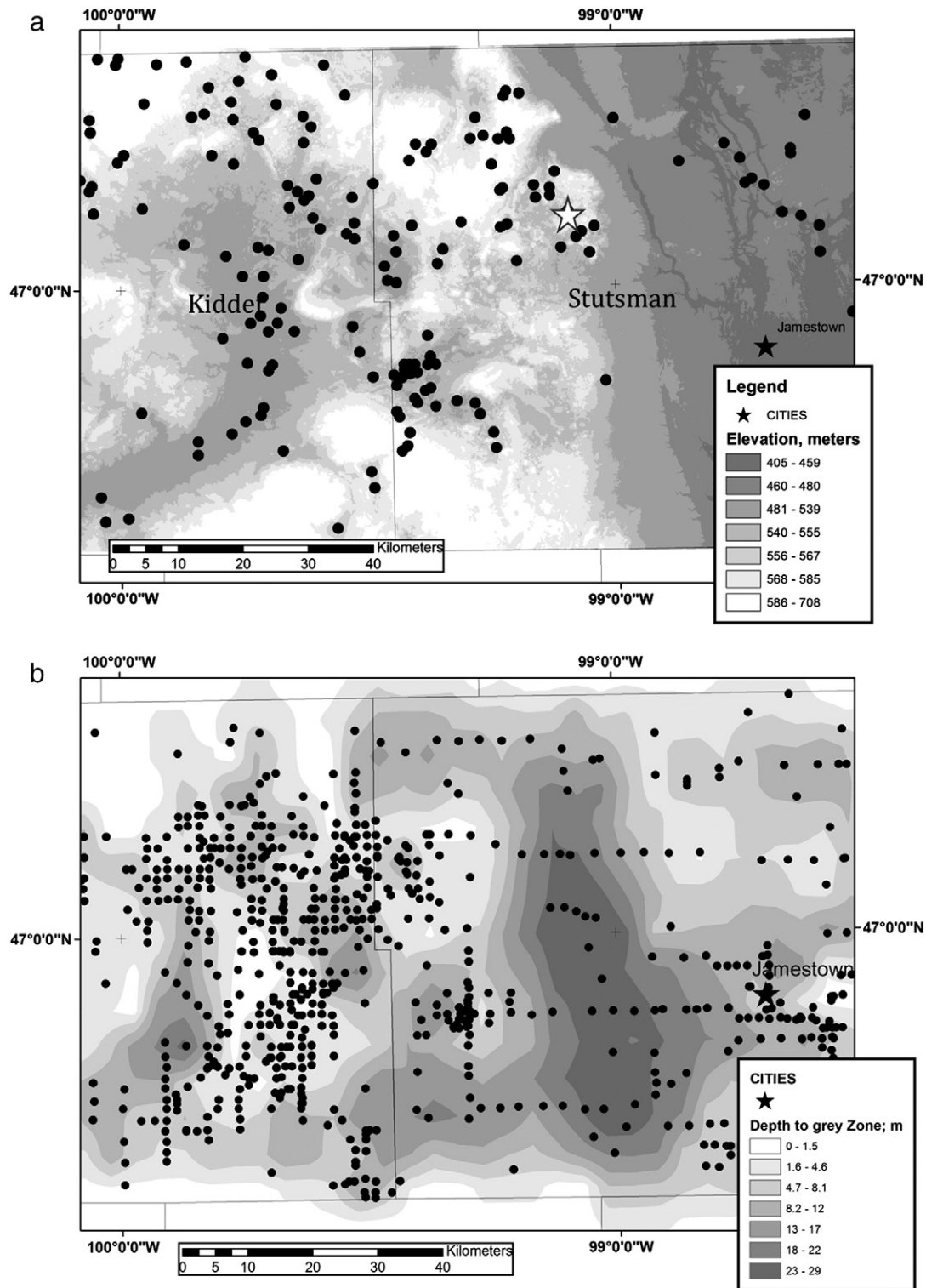


Fig. 10. (a) Map showing as black dots the location of 178 wetlands studied by Swanson et al. (1988) in a two county area that includes the CWLSA. The background is elevation as shown in the legend. (b) Black dots show the locations of test wells with data on the depth to the brown–gray transition. The star in (a) indicates the location of the CWLSA. The background is a contour plot of the depth to the brown–gray transition prepared using an inverse distance algorithm.

larger geographic areas, the process of pyrite oxidation and salt accumulation in groundwater and wetland water may develop to a greater extent than observed in the CWLSA. This seems reasonable given the potential for accumulation of SO_4^{2-} from longer groundwater fluid flow paths and larger topographic sub basins in this larger area.

As expected from the anion trend in Stutsman and Kidder County wetland water chemistry, this wider area is characterized by a zone of oxidized glacial till. In a detailed study of Stutsman County geology, Winters (1963) reported oxidation of surficial till to a brownish-yellow color and estimated that the average depth of the oxidized zone is 5.4–6.0 m. We further quantified this general observation

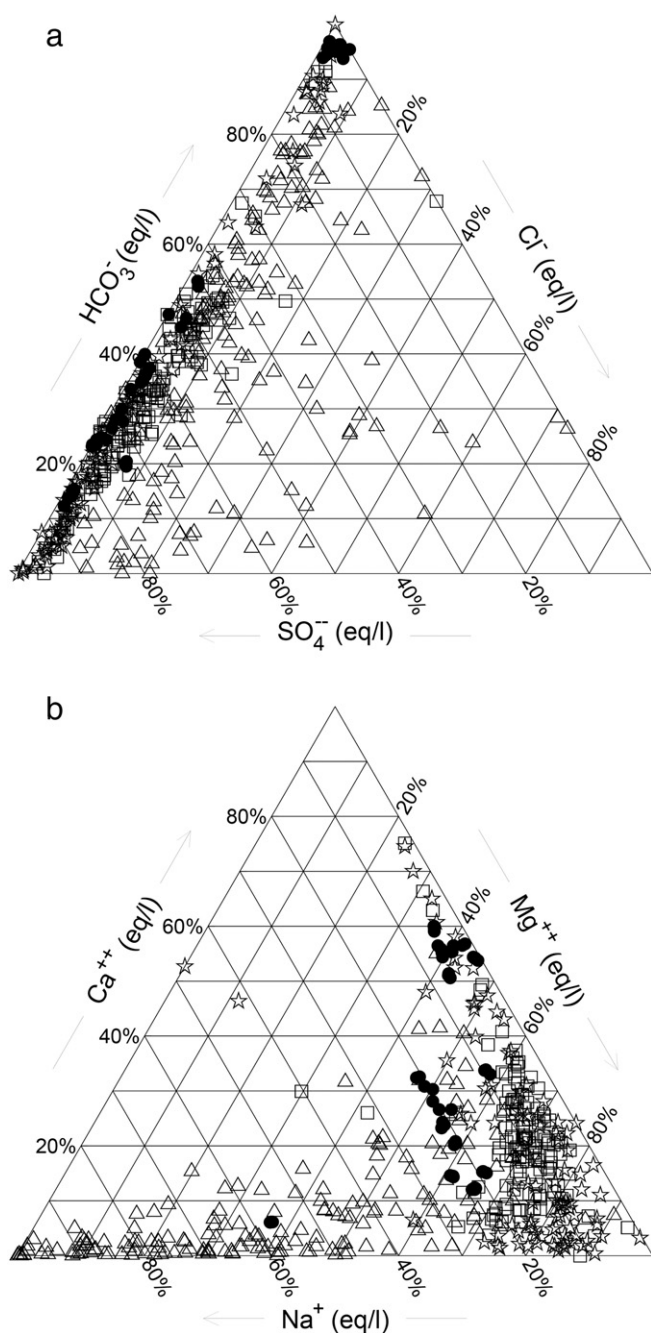


Fig. 11. Triangular plots in units of equivalents/l showing the anion (a) and cation (b) compositions of wetland waters from throughout the PPR region. Open stars represent data from 96 wetlands from the Moose Mountain area, southern Saskatchewan Canada. Open squares represent data from 79 wetlands from the Erickson-Elphinstone District, southwestern Manitoba Canada. Open triangles represent data from Swanson et al. (1988) for Stutsman and Kidder counties, North Dakota. Filled circles represent data for the CWLSA. With the exception of a subset of the Stutsman Kidder data, all samples in this geographically widespread array follow the same trend of anion evolution from HCO_3^- dominant to SO_4^{2-} dominant with increasing salinity (see also Fig. S2 that documents the increase in $\text{SO}_4^{2-}/\text{HCO}_3^-$ ratio with increasing total dissolved solids). The Canadian wetland waters tend to evolve from Ca^{2+} dominant to Mg^{2+} ($\pm \text{Na}^+$). The Stutsman and Kidder County samples are higher in Na^+ than the wetlands from the other areas.

using driller's logs for wells in the Stutsman and Kidder County area (data source <http://www.swc.nd.gov/4dlink2/4dcgi/wellsearchform/Map%20and%20Data%20Resources>). Well sites labeled as test holes in the database (Fig. 10b) were used because they were completed under the direction of the USGS and North Dakota State Water Conservation Commission and the well logs were deemed reliable.

The depth to brown–gray transition was obtained from approximately 1800 suitable logs. The oxidized brown layer appears ubiquitous throughout the two counties and extends from 1.2 to 28.2 m depth with a mean depth of 7.1 m. This is similar to the mean depth of the brown–gray transition at the CWLSA of 6.1 m. The presence of the oxidized zone is not limited to this two county area. County geologic studies by the North Dakota Geological Survey also record brown oxidized till in Ward and Sheridan counties in North Dakota (Bluemle, 1981, 1989).

4.5.2. Geochemical comparison across the prairie pothole region

The high SO_4^{2-} wetland systems driven by the oxidation of pyrite bearing glacial till we studied at the CWLSA and surrounding counties extend throughout the PPR. Canadian glacial till contains on the order of 0.1–0.3 wt.% pyrite (Keller et al., 1991; Vanstempvoort et al., 1994; Heagle et al., 2012) and Canadian pothole wetland waters show similar trends in anion and cation composition as that for the CWLSA and broader Stutsman and Kidder County wetlands. Fig. 11 (a and b) includes water analyses from 97 wetlands in the Moose Mountain area in Southern Saskatchewan Canada, occupying an area of approximately 3000 km² (Rozkowski, 1969), and 79 wetlands in the Erickson-Elphinstone district of southwestern Manitoba Canada, occupying approximately 950 km² (Barica, 1975). All of these geographically dispersed wetlands (locations shown in Fig. 1a) follow the same anion evolution pathway from HCO_3^- to SO_4^{2-} with increasing TDS. The same trend occurs in an even larger compilation of Canadian PPR wetland water chemistry data (see Last and Ginn, 2005, their Fig. 15). Furthermore, a study in the Moose Mountain area of Southern Saskatchewan Canada characterized the underlying glacial deposits. As was the case in North Dakota, there was a brown, gypsum-bearing surface layer recognized across a 15 km transect through the Moose Mountain area (Rozkowski, 1969). Additionally, the characteristic isotopically light $\delta^{34}\text{S}$ values for aqueous and solid phase SO_4^{2-} derived from marine shale pyrite oxidation that we observed in the CWLSA have also been recognized elsewhere in the PPR. Vanstempvoort et al. (1994) studied wetlands in southern Saskatchewan and southern Alberta. They reported groundwater $\delta^{34}\text{S}_{\text{sulfate}}$ values from -13.1‰ to -9‰ compared to $\delta^{34}\text{S}_{\text{pyrite}}$ values from -16‰ to -10.1‰ in underlying glacial till. Importantly, Neill and Cornwell (1992) found that isotopically light sulfur in wetland water in Manitoba Canada was incorporated into the food web.

5. Summary and conclusions

Much of the research on the PPR has focused on short-term annual to decadal processes. In this study, we have documented the long-term critical zone evolution that led to the complex geochemical characteristics of PPR wetland waters at multiple scales. By focusing initially on the hydrologically integrated 92 ha CWLSA, we were able to delineate these processes in unprecedented detail. Although previously recognized as an important process, we were able to quantify the fundamental geochemical reactions of pyrite oxidation and carbonate dissolution along a characteristic groundwater flow path using inverse geochemical modeling. We were also able to calculate the geochemical modification of groundwater that occurs, involving evaporation as well as carbonate and sulfide precipitation, which controls discharge wetland water chemistry. We estimate that these processes result in a net loss of CO_2 , a result that may be a general feature of discharge wetlands given the commonalities in geochemical evolution of wetlands throughout the region (e.g. Fig. 11a and b) with implications for regional carbon balance. Next, the quantification the total long-term oxidation of pyrite (and thus, mass of SO_4^{2-} produced) was achieved using comprehensive data sets that detailed chemical and mineralogical analyses from core samples, as well as the first comprehensive sulfur isotope data on solid and aqueous phases in such a system. These data allowed the characterization of formation of a brown oxidized upper till zone as a

proxy for the extent of pyrite oxidation. Analysis of data from well logs established the volumetric extent of this brown zone within the CWLSA, and this volume was integrated to determine the total mass of SO_4^{2-} generated. The calculated mass of SO_4^{2-} produced, approximately 10^{10} g, is much greater than that contained in CWLSA wetland waters and is now largely stored as in gypsum in the glacial till.

We utilized insights from the CWLSA study to characterize the hydrogeochemical evolution of a 9700-km² area that includes Cottonwood Lake. Because wetland waters at both spatial scales have the same trend in anionic composition, it is likely that the same processes are operating at this broader scale. Data on the regional distribution of the upper brown zone, a proxy for pyrite oxidation, derived from 1800 well logs for the larger area confirms this conclusion. Finally, we extended the results to the Canadian portion of the PPR by comparing trends in wetland water ionic composition across a broad swath of the North American PPR.

It thus appears that oxidation of a reactive pyrite-bearing component of the till derived from underlying marine shale drives many of the overall characteristics of the PPR wetlands. A vital feature of the evolution of the PPR region is the control of geologic, hydrologic, and long-term weathering processes on wetland chemistry and ecology, which makes it a prime example that illustrates the coevolution of ecosystems and landscapes in the sense of the National Research Council Report cited in the introduction (NRC, 2010).

Supplementary data to this article can be found online at <http://dx.doi.org/10.1016/j.chemgeo.2014.08.023>.

Acknowledgments

We thank George Breit for assistance with the XRD analyses and Carma San Juan for guidance with GIS analysis. We thank Caleb Balas, JoAnn Holloway, Kevin Smith, Raymond Finocchiaro, and Chip Euliss for sampling support and helpful discussions. Monique Adams and Cayce Gulbransen provided outstanding chemical analytical support. Don Rosenberry provided extremely helpful guidance with hydrology of the CWLSA. We especially want to acknowledge Tom Winter who passed away during the course of this research for his generous guidance in all matters regarding the prairie pothole region. This work was funded by the U.S. Geological Survey.

References

- Arndt, J.L., Richardson, J.L., 1989. Geochemistry of hydric soil salinity in a recharge-throughflow-discharge prairie-pothole wetland system. *Soil Sci. Soc. Am. J.* 53, 848–859.
- Arndt, J.L., Richardson, J.L., 1993. Temporal variations in the salinity of shallow groundwater from the periphery of some North Dakota wetlands (USA). *J. Hydrol.* 141, 75–105.
- Barica, J., 1975. Geochemistry and nutrient regime of saline eutrophic lakes in the Erickson-Elphenstone district of southwestern Manitoba. Tech. Rep. 511. Environment Canada, Fisheries and Marine Service, Fisheries and Marine Service, Winnipeg, Manitoba.
- Berthold, S., Bentley, L.R., Hayashi, M., 2004. Integrated hydrogeological and geophysical study of depression focused groundwater recharge in the Canadian prairies. *Water Resour. Res.* 40, W06505 (14 pp.).
- Bethke, C.M., 2008. *Geochemical and Biogeochemical Reaction Modeling*, second edition. Cambridge University Press, Cambridge England (543 pp.).
- Bischoff, W.D., Mackenzie, F.T., Bishop, F.C., 1987. Stabilities of synthetic magnesian calcites in aqueous solution: comparison with biogenic materials. *Geochim. Cosmochim. Acta* 51, 1413–1423.
- Bluemle, J.P., 1981. *Geology of Sheridan County, North Dakota*, 7th ed. North Dakota Geological Survey, Grand Forks; North Dakota (Available at: <http://www.getcited.org/pub/102274168> (Accessed January 16, 2012)).
- Bluemle, J.P., 1989. *Geology of Renville and Ward Counties, North Dakota*. North Dakota Industrial Commission, Geological Survey Division; Bulletin. 50, (Part I. 62 pp.).
- Briggs, P.H., 2002. The determination of forty elements in geological and botanical samples by inductively coupled plasma-atomic emission spectrometry. Open File Rep. 02-223-G. U.S. Geological Survey, Reston, VA.
- Briggs, P.H., Meier, A.L., 2002. The determination of forty-two elements in geological materials by inductively coupled plasma - mass spectrometry. Open File Rep. 02-223-I. U.S. Geological Survey, Reston, VA.
- Carroll, R., Pohl, G., Tracy, J., Winter, T., 2005. Simulation of a semipermanent wetland basin in the Cottonwood Lake area, East-Central North Dakota. *J. Hydrol. Eng.* 10, 70–84.
- Eberl, D.D., 2003. User Guide to RockJock-A program for determining quantitative mineralogy from x-ray diffraction data. U.S Geological Survey Open-File Report 2003-78, (47 pp.).
- Eisenlohr, W.S., 1967. Measuring evapotranspiration from vegetation-filled prairie potholes in North Dakota. *J. Am. Water Res. Assoc.* 3, 59–65.
- Euliss, N.H., Mushet, D.M., 2011. A multi-year comparison of IPCI scores for prairie pothole wetlands: implications of temporal and spatial variation. *Wetlands* 31, 713–723.
- Euliss, N.H., Wrubleski, D.A., Mushet, D.M., 1999. Wetlands of the prairie pothole region: invertebrate species composition, ecology, and management. In: Batzer, D.P., Rader, R.B., Wissinger, S.A. (Eds.), *Invertebrates in Freshwater Wetlands of North America: Ecology and Management*. John Wiley & Sons, New York, pp. 471–514.
- Euliss, N.H., Mushet, D.M., Johnson, D.H., 2002. Using aquatic invertebrates to delineate seasonal and temporary wetlands in the prairie pothole region of North America. *Wetlands* 22, 256–262.
- Euliss, N.H., LaBaugh, J.W., Friedrickson, L.H., Mushet, D.M., Laubhan, M.K., Swanson, G.A., Winter, T.C., Rosenberry, D.O., Nelson, R.D., 2004. The wetland continuum: a conceptual framework for interpreting biological studies. *Wetlands* 24, 448–458.
- Fan, Y., Miguez-Macho, G., 2011. A simple hydrologic framework for simulating wetlands in climate and earth system models. *Clim. Dyn.* 37, 253–278.
- Freeze, R.A., Cherry, J.A., 1979. *Groundwater*. Invertebrates in Freshwater Wetlands of North America: *Ecology and Management*. Prentice-Hall, Inc., Englewood Cliffs, NJ, (604 pp.).
- Gautier, D.L., 1987. Isotopic composition of pyrite: relationship to organic matter type and iron availability in some North American cretaceous shales. *Chem. Geol. Isot. Geosci. Sect.* 65, 293–303.
- Giesemann, A., Jager, H.J., Norman, A.L., Krouse, H.R., Brand, W.A., 1994. On-line sulfur-isotope determination using an elemental analyzer coupled to a mass spectrometer. *Anal. Chem.* 66, 2816–2819.
- Goldhaber, M.B., 2004. Sulfur-rich Sediments. In: Holland, H.D., Turekian, K.K. (Eds.), *Treatise on Geochemistry*, vol. 7. Elsevier, Amsterdam, pp. 257–288.
- Heagle, D., Hayashi, M., van der Kamp, G., 2007. Use of solute mass balance to quantify geochemical processes in a prairie recharge wetland. *Wetlands* 27 (4), 806–818.
- Heagle, D., Hayashi, M., van der Kamp, G., 2012. Surface-subsurface salinity distribution and exchange in a closed basin prairie wetland. *J. Hydrol.* 478 (25), 1–14.
- Hendry, M.J., Cherry, J.A., Wallick, E.L., 1986. Origin and distribution of sulfate in a fractured till in southern Alberta, Canada. *Water Resour. Res.* 22, 45–61.
- Jones, B. and D. Deocampo (2003), Geochemistry of saline lakes, in *Treatise on Geochemistry*, vol. 5, pp.393–424, Volume 5 Ed. James I. Drever, Executive Editors, H.D. Holland and K.K. Turekian.
- Kantrud, H.A., Krapu, G.L., Swanson, G.A., 1989. Prairie basin wetlands of the Dakotas: a community profile. *U.S. Fish Wildl. Serv. Biol. Rep.* 85 (7.28) (116 pp.).
- Keller, C.K., Van Der Kamp, G., Cherry, J.A., 1989. A multiscale study of the permeability of a thick clayey till. *Water Resour. Res.* 25 (11), 2299–2317.
- Keller, C. Kent, Van der Kamp, G., Cherry, J., 1991. Hydrogeochemistry of a clayey till 1. Spatial variability. *Water Resour. Res.* 27 (10), 2543–2554.
- LaBaugh, J.W., 1989. Chemical characteristics of water in northern prairie wetlands. In: van der Valk, A.G. (Ed.), *Northern prairie wetlands*. Iowa State University Press, pp. 56–90.
- LaBaugh, J.W., Winter, T.C., Swanson, G.A., Rosenberry, D.O., Nelson, R.D., Euliss, N.H., 1996. Changes in atmospheric circulation patterns affect mid-continent wetlands sensitive to climate. *Limnol. Oceanogr.* 41, 864–870.
- LaBaugh, J.W., Winter, T.C., Rosenberry, D.O., 1998. Hydrologic functions of prairie wetlands. *Great Plains Res.* 8, 17–37.
- Last, W.M., 1999. Geolimnology of the Great Plains of western Canada. *Geol. Surv. Can. Bull.* 534, 23–53 (Available at: <http://home.cc.umanitoba.ca/~mlast/publications/page1/assets/1999geolim.pdf> (Accessed June 30, 2011)).
- Last, W.M., Ginn, F.M., 2005. Saline systems of the Great Plains of western Canada: an overview of the limnology and paleolimnology. *Saline Syst.* 1 (c), 10 (Available at: <http://www.pubmedcentral.nih.gov/articlerender.fcgi?artid=1315329&tool=pmcentrez&rendertype=abstract> (Accessed November 24, 2010)).
- Lissey, A., 1971. Depression-focused transient ground water flow patterns in Manitoba. *Geol. Assoc. Can. Spec. Pap.* 9, 333–341.
- Mills, C.T., Goldhaber, M.B., Stricker, C.A., Holloway, J.M., Morrison, J.M., Ellefsen, K.J., Rosenberry, D.O., Thurston, R.S., 2011. Using stable isotopes to understand hydrochemical processes in and around a prairie pothole wetland in the Northern Great Plains, USA. *Appl. Geochem.* 26, S97–S100.
- Muller, G., Irion, G., Forstner, U., 1972. Formation and diagenesis of inorganic Ca–Mg carbonates in the lacustrine environment. *Naturwissenschaften* 59, 158–164.
- Nachshon, U., Ireson, A., van der Kamp, G., Wheeler, H., 2013. Sulfate salt dynamics in the glaciated plains of North America. *J. Hydrol.* 499, 188–199.
- National Research Council's Committee on Basic Research Opportunities in the Earth Sciences, 2001. *Basic Research Opportunities in the Earth Sciences*. National Academies Press, Washington D.C.
- Neill, C., Cornwell, J., 1992. Stable carbon, nitrogen, and sulfur isotopes, in a prairie marsh food web. *Wetlands* 12, 217–224.
- NRC, 2010. *Landscapes on the Edge: New Horizons for Research on Earth's Surface*. National Academies Press, (180 pp.).
- Ohmoto, H., Goldhaber, M., 1997. Applications of Sulfur and Carbon Isotopes in Ore Deposit Research. In: Barnes, H. (Ed.), *The Geochemistry of Hydrothermal Ore Deposits*, third edition, pp. 517–612.
- Plummer, L.N., Parkhurst, D.L., Thorstenson, D.C., 1983. Development of reaction models for ground-water systems. *Geochim. Cosmochim. Acta* 47, 665–685.
- Rosenberry, D.O., Winter, T.C., 1997. Dynamics of water-table fluctuations in an upland between two prairie-pothole wetlands in North Dakota. *J. Hydrol.* 191, 266–289.

- Rosenberry, D.O., Stannard, D.I., Winter, T.C., Martinez, M.L., 2004. Comparison of 13 equations for determining evapotranspiration from a prairie wetland, Cottonwood Lake area, North Dakota, USA. *Wetlands* 24 (3), 483–497.
- Rozkowski, A., 1969. Chemistry of ground and surface waters in the Moose Mountain area, southern Saskatchewan. *Geol. Surv. Can. Pap.* 67–9, 71p.
- Sloan, C.E., 1972. Ground-water hydrology of prairie potholes in North Dakota. *U. S. Geol. Surv. Prof. Pap.* 585-C (Washington, D.C.).
- Smith, D.B., Woodruff, L.G., O'Leary, R.M., Cannon, W.F., Garrett, R.G., Kilburn, J.E., Goldhaber, M.B., 2009. Pilot studies for the North American Soil Geochemical Landscapes Project—Site selection, sampling protocols, analytical methods, and quality control protocols. *Appl. Geochem.* 24, 1357–1368.
- Stets, E.G., Striegl, R.G., Aiken, G.R., Rosenberry, D.O., Winter, T.C., 2009. Hydrologic support of carbon dioxide flux revealed by whole-lake carbon budgets. *J. Geophys. Res.* 114, G01008 (14 pp.).
- Stewart, R., Kantrud, H., 1972. Vegetation of prairie potholes, North Dakota, in relation to quality of water and other environmental factors. *U. S. Geol. Surv. Prof. Pap.* 585-D (Washington, D.C., Available at: <http://library.ndsu.edu/exhibits/text/potholes/585d.html> (Accessed January 16, 2012)).
- Swanson, G.A., 1978. A water column sampler for invertebrates in shallow wetlands. *J. Wildl. Manag.* 42, 670–671.
- Swanson, K.D., 1990. Chemical evaluation of ground-water in clay till in a prairie wetland setting in the Cottonwood Lake area, Stutsman County, North Dakota (M.S. thesis) Dep. Of Geology, University of Wisconsin, Madison, WI.
- Swanson, G.A., Winter, T.C., Adomaitis, V.A., LaBaugh, J.W., 1988. Chemical Characteristics of Prairie Lakes in South-central North Dakota. Their Potential for Influencing Use by Fish and Wildlife. U.S. Fish and Wildlife Service, Technical Report. 18. Department of the Interior, Fish and Wildlife Service, Washington D.C. USA.
- Swanson, G.A., Euliss, N.H., Hanson, B.A., Mushet, D.M., 2003. Dynamics of a prairie pothole wetland complex: implications for wetland management. *U. S. Geol. Surv. Prof. Pap.* 1675, 55–94.
- Taggart Jr., J.E., 2002. Analytical methods for chemical analysis of geologic and other materials. U.S. Geological Survey, USGS Open-File Report 02-0223. (20 pp.).
- Tuttle, M.L., Goldhaber, M.B., Williamson, D.L., 1986. An analytical scheme for determining forms of sulphur in oil shales and associated rocks. *Talanta* 33, 953–961.
- van der Kamp, G., Hayashi, M., 1998. The groundwater recharge function of small wetlands in the semi-arid northern prairies. *Great Plains Res.* 8, 39–56.
- van der Kamp, G., Hayashi, M., 2009. Groundwater-wetland ecosystem interaction in the semiarid glaciated plains of North America. *Hydrogeol. J.* 17, 203–214.
- van der Valk, A.G., Pederson, R.L., 2003. The swancc decision and its implications for prairie potholes. *Wetlands* 23 (3), 590–596.
- Van Stempvoort, D., Hendry, M.J., Schoenau, J.J., Krous, H.R., 1994. Sources and dynamics of sulfur in weathered till, Western Glaciated Plains of North America. *Chem. Geol.* 111, 35–56.
- Wallick, E.I., 1981. Chemical evolution of groundwater in a drainage basin of Holocene age, east-central Alberta. *J. Hydrol.* 54, 245–283.
- Whittaker, S., Kyser, T., 1990. Effects of sources and diagenesis on the isotopic and chemical composition of carbon and sulfur in Cretaceous shales. *Geochim. Cosmochim. Acta* 54, 2799–2810.
- Winter, T.C., 2003. Hydrological, chemical, and biological characteristics of a prairie pothole wetland complex under highly variable climate conditions - the Cottonwood Lake area, east-central North Dakota. *U. S. Geol. Surv. Prof. Pap.* 1675, 1–24.
- Winter, T.C., Carr, M.R., 1980. Hydrologic Setting of Wetlands in the Cottonwood Lake Area, Stutsman County, North Dakota. *U.S. Geol. Surv. Water Res. Invest. Report.* pp. 80–99.
- Winter, T.C., Rosenberry, D.O., 1998. Hydrology of prairie pothole wetlands during drought and deluge: a 17-year study of the Cottonwood Lake Wetland Complex in North Dakota in the perspective of longer term measured and proxy hydrological records. *Clim. Chang.* 40, 189–209.
- Winters, H.A., 1963. Geology and ground water resources of Stutsman County; North Dakota, Part I, North Dakota Geology, North Dakota. *Geol. Surv. Bull.* 41 (1) (84 pp.).
- Zeng, T., Arnold, W.A., Toner, B.M., 2013. Microscale Characterization of Sulfur Speciation in Lake Sediments. *Environ. Sci. Technol.* 47, 1287–1296.